Nonlinear interaction of an acoustical wave with a counter-propagating weak shock

François Coulouvrat, Ronan Delalande, Mathieu Ducousso

Nonlinear interaction of an acoustical wave with a counter-propagating weak shock

François Coulouvrat,[1,a] Ronan Delalande,[1,2] and Mathieu Ducousso[2,3]

[1]*Sorbonne Université - CNRS - Institut Jean Le Rond d'Alembert - F-75005 Paris - France*

[2]*PIMM Laboratory - UMR 8006 - Arts et Metiers Institute of Technology (ENSAM) - CNRS - Cnam - 151 boulevard de l'Hôpital - 75013 Paris (France)*

[3]*Safran Tech - Rue des Jeunes Bois - Châteaufort - 78772 Magny-les-Hameaux - France*

During its propagation, a shock wave may come across and interact with different perturbations, including acoustical waves. While this issue been the subject of many studies, the particular acoustic-acoustic interaction between a weak shock and a sound wave has been very scarcely investigated. Here a theory describing the encounter of those two waves is developed, up to second- and third-order. According to the incidence angle and shock strength, several regimes of acoustic transmission through the shock are identified. Generation of entropy as well as vorticity modes are determined, while the perturbation of the shock front by the acoustic wave is quantified. The theory predicts strongly different behaviors between air and water, and preliminary results are coherent with recent experimental observations in solids. It paves the way to both an acoustic monitoring of shock wave as well as a method to determine the quadratic and cubic nonlinear parameters of material.

[a]francois.coulouvrat@sorbonne-universite.fr

I. INTRODUCTION

Shock wave interaction with ambient flow is an issue studied for long by many authors, however mostly for the case of relatively strong shocks in perfect gases. The present paper generalizes these studies to any ideal fluid properties, and focuses on the 'acoustic-acoustic' interaction between a wave of infinitesimal small amplitude and a shock of small amplitude. This allows to obtain several analytical results revealing the dimensionless fluid properties that are important for the transmission of acoustic waves through a weak shock.

In his seminal work, Burgers[1,2] investigated theoretically the one-dimensional transmission of a sound wave impinging normally a stationary shock wave. He namely pointed out there cannot be any reflected wave, as this one would move slower than the flow. Similarly, when considering, as in the present paper, a shock moving at a necessarily supersonic speed in an undisturbed medium and interacting with a counter-propagating sound wave, a reflected wave propagating at the speed of sound would immediately be overwhelmed by the shock. However, Burgers pointed out that, for properly solving the problem, one has to consider also the existence of an entropy mode behind the shock, and an oscillation of the shock front induced by its interaction with the sound wave. This leads to three unknowns (the amplitudes of the transmitted sound wave, entropy mode and shock perturbation) that are fully determined by the three Rankine-Hugoniot relations for mass, momentum and energy conservation through a shock. Though solving mathematically the problem for the case of a perfect gas, Burgers did not analyze his results. Note that Blokhintzev in his independent study[3] also showed the absence of reflection but did not took into account the shock oscillation. A close approach was followed by Kantrowitz[4] who investigated mostly the stability of shock waves. The two-dimensional case was studied a few years later, first, to our knowledge, by Moore[5]. This author pointed out a vorticity perturbation behind the shock has also to be considered (which was ignored by Brillouin[6]), both vorticity and entropy modes being non-propagating modes simply convected by the flow behind the shock[7]. He also outlined that an acoustical wave propagating in the region behind the shock and towards it (at a speed necessarily faster than the shock speed) cannot be transmitted to the unperturbed fluid ahead of the shock. Therefore, the supersonic region behind the shock appears as a ”sonic black hole” : any sound wave entering this region cannot escape it. This opened a fruitful analogy between sound/shock waves interaction and gravitational black holes[8]. Experimental realization of such a sonic black hole for a Bose-Einstein condensate[9] lead to the recent first laboratory experimental observation of Hawking radiation[10] (thermal black-body radiation out of a black hole's event horizon that causes its evaporation). Another application of sound/shock interaction was proposed by McKenzie and Westphal[11] who, apparently unaware of the work of Moore, generalized Burgers' work at 2D. Their theory has been verified by direct numerical simulations [12]. They also extended it to the interaction between Alfvén waves and hydromagnetic shocks, as a model for solar wind interacting with earth magnetopause viewed as a magnetic bow shock[13]. This problem was previously examined by Kontorovich[14] who also outlined the Doppler frequency shift undergone by the sound wave. Such kind of models has also been applied to the problem of cosmic rays acceleration by shock waves associated with supernova remnants[15]. McKenzie and Westphal[11] also pointed out that, irrespective of its nature, either a sound, an entropy or a vorticity mode interacting with a shock, generates all three modes behind it. Associated to the work of Kantrowitz, this observation paved the way to an abundant literature investigating shock interaction with turbulence (e.g. a vorticity field), shock stability and supersonic boundary layer receptivity that finds multiple applications in aerodynamics. A literature review of this problem is beyond the scope of this paper, the reader is referred to Andreopoulos's review *et al.*[16] or, regarding receptivity, to the work of Ma and Zhong[17]. Considering specifically the interaction of an acoustical field with a shock, a numerical analysis performed in air over a wide range of Mach numbers between 1 and 5 by Mahesh *et al.*[18] recovered the theoretical observations of Moore[5]: below a critical angle of incidence, the transmitted sound wave is propagating, while it is exponentially decaying above. In this last case, the incident sound energy is transferred to the vorticity field. For weak or moderate shocks (Mach number below approximately 1.2) and an isotropic field (all directions of incidence) the far field kinetic energy of the acoustical field slightly increases, while it decreases for larger values (between 1.2 and 1.8) and then increases again. The kinetic energy of the vorticity field increases monotonously with the Mach number, and exceeds the acoustic one for Mach about 2.25 (see their Figure 8). Entropy fluctuations become significant only above Mach 1.5 (see their Figure 10).

The case of sound interaction with either weak shocks or in other materials has received little attention. In solids, we can mention the theoretical works of Morro[19] and Pluchino[20]. A recent experimental interaction[21] between a laser-generated shock wave and a counter-propagating ultrasonic field put in evidence a strong interaction between the two waves in either aluminium, titanium and water, with an amplitude loss for the ultrasound wave up to about 10%, even though the shock amplitude is relatively low. This motivated our present study, focused on the almost unexplored case of acoustical weak shocks in any type of common fluids. Indeed, weak shocks are substantially different from both strong shocks and from linear sound waves. Their entropy variations are not null but remain much smaller than those of all other variables, of order ϵ^3 versus ϵ if ϵ is a small dimensionless parameter measuring the shock amplitude[22]. Also, their reflection on surfaces neither satisfies the linear Snell-Descartes laws nor follows the strongly nonlinear Mach reflection[23]. We expect this 'in-between' behavior to induce specific features in case of interaction with a linear sound wave. Moreover, compression weak shocks in common fluids such as air and water (or in hyperelastic solids) can be described mechanically by a single dimensionless thermo-mechanical parameter of nonlinearity β, thus allowing to study with a unified formalism the behaviors of gases and liquids, and also of solids in the 1D case (otherwise shear elastic waves also have to be considered in solids).

In the present work, the interaction of a weak shock wave with an incident acoustic wave is investigated for any common fluid, either liquid or gaseous. The various quantities describing the propagation of the weak shock are described in section two. Weak shock limit is reexamined by performing asymptotic expansions relative to small amplitude parameter ϵ one order higher (order three instead of order two). The acoustic incident and transmitted fields, as well as the entropy and vorticity modes and shock perturbation are introduced in the following section three. The sound wave refraction and its Doppler frequency shift resulting from the interaction are highlighted in section four which investigates in details the various regimes of sound transmission. The amplitudes of the various modes are determined in the fifth section. Throughout the entire paper, cases of air and water are compared. For those two fluids, results obtained from second- and third-order theories are systematically compared to quantify the limits of weak shock approximation.

II. THE UNPERTURBED WEAK SHOCK

In a perfect fluid with negligible viscosity and heat conduction, pressure $p(x,y,t)$, density $\rho(x,y,t)$, speed of sound $c(x,y,t)$, flow velocity $\boldsymbol{v}(x,y,t)$, specific entropy $s(x,y,t)$, temperature $T(x,y,t)$ and specific enthalpy $h(x,y,t)$ satisfy the Euler equations of mass, momentum and energy balance in addition to the medium constitutive state equation. Rankine-Hugoniot (RH) jump relations describe the mass, momentum and energy balance through a shock moving with velocity $\boldsymbol{w}$

$$w_n\left(\rho_+ - \rho_-\right) = (\rho v_n)_+ - (\rho v_n)_- \tag{1}$$

$$w_n\left((\rho v_n)_+ - (\rho v_n)_-\right) = (p + \rho v_n^2)_+ - (p + \rho v_n^2)_- \tag{2}$$

$$(v_t)_+ = (v_t)_- \tag{3}$$

$$h_+ + \frac{1}{2}\left((v_n)_+ - w_n\right)^2 = h_- + \frac{1}{2}\left((v_n)_- - w_n\right)^2 \tag{4}$$

where index $_+$ (resp. index $_-$) denotes the value of any quantity q immediately behind (resp. ahead of) the shock. For velocity vectors $\boldsymbol{v}$ and $\boldsymbol{w}$, indexes $_n$ and $_t$ are respectfully indicating their normal (for instance $v_n = \boldsymbol{v}.\boldsymbol{n}$) and tangential component to the shock front with $\boldsymbol{n}$ the wave front normal vector, oriented towards the unperturbed region.

As illustrated in Fig.(1), a weak step shock at position $x_s(t)$ propagates with speed $\boldsymbol{w_s} = (dx_s/dt)\boldsymbol{e_x}$, separating the fluid into two homogeneous but distinct regions. The

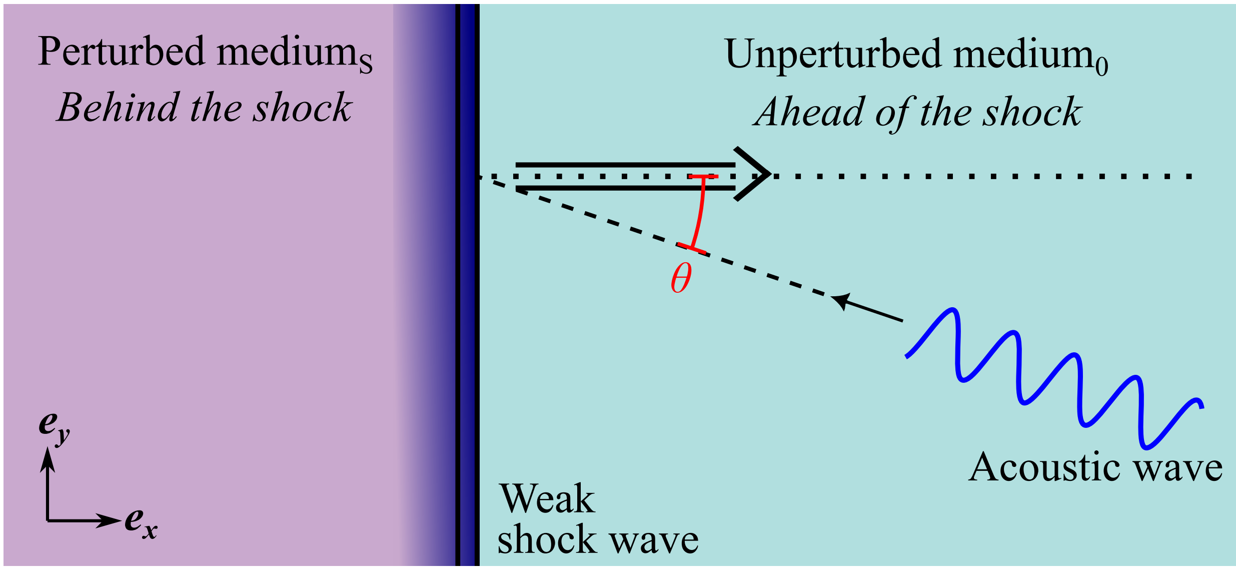

FIG. 1. Interaction geometry

frame of reference is chosen so that the fluid ahead of the shock is at rest, implying $\boldsymbol{v}_0 = \mathbf{0}$. Behind the shock the homogeneous flow is noted $\boldsymbol{v_s} = v_s \boldsymbol{e_x}$. In this case, the RH relations (1-4) reduce to

$$w_s(\rho_0 - \rho_s) = -\rho_s v_s, \tag{5}$$

$$-w_s \rho_s v_s = p_0 - (p_s + \rho_s v_s^2), \tag{6}$$

$$h_0 + \frac{1}{2} w_s^2 = h_s + \frac{1}{2}(v_s - w_s)^2 \, . \tag{7}$$

The shock wave is assumed to be of weak amplitude, measured by the parameter $\epsilon \ll 1$ as a dimensionless density jump $\rho_s - \rho_0 = \rho_0 \, \epsilon$. In this case, it is well-known[24] that the entropy jump is of very small order ϵ^3 and is therefore negligible at leading order

$$s_s - s_0 = \epsilon^3 \frac{c_0^2}{6T_0} \left(1 + \frac{B}{2A}\right) \tag{8}$$

This relation[22] involves the quadratic nonlinear parameter of the fluid given by

$$\frac{B}{2A} = \frac{1}{2}\frac{\rho_0}{c_0^2}\left(\frac{\partial^2 p}{\partial \rho^2}\right)_s (\rho_0, s_0). \tag{9}$$

It is equal to $(\gamma - 1)/2$ for a perfect gas of specific heats ratio γ. For diatomic gases such as air $\gamma = 1.4$ and $B/2A = 0.2$. Another commonly used quadratic nonlinear parameter is $\beta = 1 + B/2A$, which combines the influence of both convection and equation of state for a nonlinear simple wave.

The equation of state for a common fluid $p = p(\rho, s)$ and the sound speed $c = (\partial p/\partial \rho)_s$ can thus be expanded behind the shock up to third order

$$p_s = p_0 + \rho_0 c_0^2 \left[\epsilon + \frac{B}{2A}\epsilon^2 + \frac{C}{6A}\epsilon^3 + \left(\rho_0 c_0^2 \left(\frac{\partial p}{\partial s}\right)_\rho (\rho_0, s_0)\right)(s - s_0) + O(\epsilon^4)\right] \tag{10}$$

and

$$c_s = c_0 \left[1 + \frac{B\epsilon}{2A} + \frac{1}{8}\left(\frac{2C}{A} - \left(\frac{B}{A}\right)^2\right)\epsilon^2 + O(\epsilon^3)\right]. \tag{11}$$

In the r.h.s. of Eq.(10) the first three terms correspond to the third-order expansion of isentropic pressure variation with density. Cubic nonlinear effects involve the nonlinear parameter $C/6A$ where

$$\frac{C}{6A} = \frac{1}{6}\frac{\rho_0^2}{c_0^2}\left(\frac{\partial^3 p}{\partial \rho^3}\right)_s (\rho_0, s_0). \tag{12}$$

For a perfect gas, one has $C/6A = (\gamma - 1)(\gamma - 2)/6$. Therefore $C/6A = -0.04$ for any diatomic gases such as air. For water at 20°C, $B/A = 4.96$ and $C/6A = 36.95$[25]. The last term in the r.h.s. of Eq.(10) is associated to non-isentropic effects, which involve only the first-order, linear entropy variation according to Eq.(8). Therefore Eq.(10) can be rewritten

$$p_s = p_0 + \rho_0 c_0^2 \left[\epsilon + \frac{B}{2A}\epsilon^2 + K\epsilon^3 + O(\epsilon^4) \right] \tag{13}$$

with $K = C/6A + D$. Coefficient D

$$D = \frac{k}{\rho_0 c_0^2} \left(\frac{\partial p}{\partial s} \right)_\rho (\rho_0, s_0), \tag{14}$$

where $k = (s_s - s_0)/\epsilon^3$ measures the influence of the entropy jump on the pressure jump, which cannot be neglected at third order.An expression for D is provided in Appendix A. According to the usual terminology[24], a weak shock is defined as a shock of sufficiently small amplitude so that entropy variations can be neglected. Hence it corresponds to the second-order expansion of pressure Eq.(13) up to order $O(\epsilon^2)$. To be consistent, a third-order expansion up to order $O(\epsilon^3)$ includes necessarily entropy effects and is here referred to as a shock of moderate amplitude.

The ratio of mass Eq.(5) and momentum Eq.(6) relations eliminates the shock speed and yields after substitution of the pressure Eq.(13) the expansion for the flow velocity behind the shock

$$v_s = \epsilon c_0 \left[1 + \frac{\epsilon}{2}\left(\frac{B}{2A} - 1 \right) \right. \\ \left. + \frac{\epsilon^2}{2}\left(\frac{3}{4} - \frac{B}{4A} - \frac{1}{4}\left(\frac{B}{2A} \right)^2 + K \right) + O(\epsilon^4) \right]. \tag{15}$$

The shock speed can now be deduced from this expression and the mass RH equation Eq.(5)

$$w_s = c_0 \left[1 + \frac{\epsilon}{2}\left(\frac{B}{2A} + 1 \right) \right. \\ \left. + \frac{\epsilon^2}{2}\left(-\frac{1}{4} + \frac{B}{4A} - \frac{1}{4}\left(\frac{B}{2A} \right)^2 + K \right) + O(\epsilon^3) \right]. \tag{16}$$

Eq.(16) recovers the classical result for the second order (weak shock) approximation $w_s = (c_0 + c_s + v_s)/2 + O(\epsilon^2)$: the shock velocity of a weak shock is the average of the speeds of sound ahead of (c_0) and behind ($c_s + v_s$) the shock, this last one taking into account the influence of flow convection. This result is not valid any more when considering higher order terms (here cubic ones). The energy RH relation finally leads to Eq.(8) for the entropy jump. It is not reproduced here as it can be found in classical textbooks.

III. THE FIELD OF PERTURBATIONS

A. The incident acoustic wave

As sketched in Fig.(1), an acoustic wave propagates ahead of the shock and towards it with an incident angle θ relative to the unperturbed shock normal vector. The frame of reference is unchanged relative to the unperturbed case. Considering a harmonic decomposition, the density perturbation due to this wave is

$$\rho_A^{inc}(x > x_s, y, t) \;=\; A \exp\left[j(k_{x,A}^{inc} x \;+\; k_{y,A}^{inc} y \;-\; \omega t)\right] \tag{17}$$

with A its amplitude assumed to be much smaller than the entropy jump $A \ll \epsilon \rho_0$, ω the angular frequency and $k_{z,A}^{inc}$ the component of the wave vector along the $\boldsymbol{e}_z$ direction with $z = (x, y)$. In the considered geometry we have $\boldsymbol{k}_A^{inc} = (k_{x,A}^{inc}\,,\, k_{y,A}^{inc}) = (\omega/c_0)(-\cos\theta\,,\, \sin\theta)$. The acoustical perturbations of the pressure, velocity and entropy field are $p_A^{inc} = c_0^2 \rho_A^{inc}$, $\boldsymbol{v}_A^{inc} = c_0(\rho_A^{inc}/\rho_0)(-\cos\theta, \sin\theta)$ and $s_A^{inc} = 0$.

B. The modes behind the shock

As the shock wave is propagating with a velocity w_s greater than the speed of sound c_0 ahead of the shock no reflected wave is possible on this side. Behind the shock, the possible modes are obtained by linearizing Euler equations around the ambient uniform flow of pressure p_s and density ρ_s moving at velocity $\boldsymbol{v}_s = v_s \boldsymbol{e}_x$. This leads to three types of solutions : a transmitted acoustic wave, a vorticity mode and an entropy one - respectively indexed by ${}^{tr}_{A}$, ${}_{V}$ and ${}_{E}$. For each one, a dimensionless transmission coefficient in amplitude T_A^{tr}, T_V or T_E is introduced. To satisfy the RH relations on the shock surface, all modes should have the same spatial dependence along $\boldsymbol{e}_y$ implying $k^{inc}_{A,y} = k_{E,y} = k_{V,y} = k^{tr}_{A,y} = k_y$. The adiabatic ($s^{tr}_A = 0$) perturbation due to the acoustic transmitted wave can then be expressed

$$\rho^{tr}_A = AT_A \exp[j(k^{tr}_{A,x}x + k_y y - \omega^{tr}_A t)], \tag{18}$$

$$p^{tr}_A = AT_A c_s^2 \exp[j(k^{tr}_{A,x}x + k_y y - \omega^{tr}_A t)], \tag{19}$$

$$\boldsymbol{v}^{tr}_A = AT_A \frac{c_s}{\rho_s} \boldsymbol{n}^{tr}_A \exp[j(k^{tr}_{A,x}x + k_y y - \omega^{tr}_A t)]. \tag{20}$$

Here ω^{tr}_A is the transmitted angular frequency, different from the incident one due to the Doppler effect induced by the sound interaction with the moving shock front (frequency is not Galilean-invariant). The transmitted acoustic wave vector

$$\boldsymbol{k}^{tr}_A = \omega^{tr}_A \boldsymbol{r}^{tr}_A \ . \tag{21}$$

satisfies the acoustical dispersion relation in a fluid of sound speed c_s convected by the flow at speed $\boldsymbol{v}_s = (v_s, 0)$

$$c_s^2\left(\boldsymbol{k}_A^{tr}\right)^2 = (\omega_A^{tr} - \boldsymbol{v}_s.\boldsymbol{k}_A^{tr})^2 \Leftrightarrow k_A^{tr} = \frac{\omega_A^{tr}}{c_s + \boldsymbol{v}_s.\boldsymbol{n}_A^{tr}} \tag{22}$$

with $\boldsymbol{n}_A^{tr}$ the unit vector directing the transmitted wave and $\boldsymbol{r}_A^{tr}$ the slowness vector of the transmitted wave. The perturbations associated to the vorticity and entropy modes are similarly expressed

$$(\rho_V, p_V, v_{x,V}, v_{y,V}, s_V) \;=\; T_V \frac{c_s}{\rho_s}\Big(0, 0, -v_s k_y/\omega_V, 1, 0\Big) \\ \times A \exp[i(k_y y \;-\; \omega_V(t - x/v_s)] \tag{23}$$

and

$$(\rho_E, p_E, v_{x,E}, v_{y,E}, s_E) \;=\; T_E\Big(1, 0, 0, 0, -c_s^2(\partial p/\partial s)^{-1}\Big) \\ \times A \exp[i(k_y y \;-\; \omega_E(t - x/v_s)]\;. \tag{24}$$

The vorticity mode is a pure rotational, velocity field with no associated perturbation of pressure, density nor entropy. The ratio c_s/ρ_s in Eq.(23) is chosen to make the coefficient T_V dimensionless. On the contrary, the entropy mode is a perturbation of density and entropy only, leaving pressure and velocity unaffected. Both vorticity and entropy fluctuations are simply convected by the ambient flow speed v_s but do not propagate. We note q_P the total perturbation of any quantity q in the post-shock region

$$q_P \;=\; q_A^{tr} \;+\; q_E \;+\; q_V\;. \tag{25}$$

C. The shock front perturbation

Due to the incident acoustic field, the shock front itself is perturbed and cannot be considered as perfectly plane anymore. Therefore a correction is applied on the shock position along time

$$x_c(y,t) \;=\; x_s \;+\; f(y,t) \;=\; w_s t \;+\; f(y,t) \tag{26}$$

where $f(y,t)$ is proportional to the incident acoustic amplitude A. Thanks to this smallness approximation, the vector normal to the shock front is $\boldsymbol{n} = (1, -\partial f/\partial y)/\sqrt{1+(\partial f/\partial y)^2} \approx (1, -\partial f/\partial y)$, the vector tangential to the shock front is $\boldsymbol{t} = (\partial f/\partial y, 1)/\sqrt{1+(\partial f/\partial y)^2} \approx (\partial f/\partial y, 1)$ and the normal shock velocity is $w_n = w_s + \partial f/\partial t$. Velocity $w_A = \partial f/\partial t$ is therefore the perturbation of the shock front normal velocity resulting from its interaction with the incident sound wave. It must be proportional to the common exponential form $\exp(jk_y y)$ leading to

$$w_A \;=\; \frac{w_s}{\rho_0} T_W A \exp\left(j\frac{\omega}{c_0}\left[\sin\theta y \;-\; (c_0 \;+\; w_s\cos\theta)t\right]\right). \tag{27}$$

The time dependence is the one of the incident wave on the shock front position $x_s = w_s t$ (see later on) and T_W is a dimensionless amplitude coefficient. We deduce

$$f(y,t) \;=\; \frac{jc_0 w_s}{\rho_0\omega(c_0 \;+\; w_s\cos\theta)} \times T_W A \exp\left(j\frac{\omega}{c_0}\left[\sin\theta y \;-\; (c_0 \;+\; w_s\cos\theta)t\right]\right). \tag{28}$$

IV. REFRACTION AND DOPPLER EFFECT

A. Linearization of jump relations

Ahead of the shock, any quantity q calculated on the actual shock front is the sum of the homogeneous, unperturbed ambient flow q_0 and of the incident acoustic field q_A^{inc}. One deduces the following linearization

$$\begin{aligned} q_+(\boldsymbol{x}_c(t),t) &= (q_0 + q_A^{inc})_+(w_s t + f, y_c, t) \\ &= q_0 + q_A^{inc}(w_s t, y_c, t). \end{aligned} \tag{29}$$

Similarly one has behind the shock

$$\begin{aligned} q_-(\boldsymbol{x}_c(t),t) &= (q_s + q_P)_+(w_s t + f, y_c, t) \\ &= q_s + q_P(w_s t, y_c, t), \end{aligned} \tag{30}$$

while we recall that shock velocity $w_n = w_s + w_A$. Perturbations q_P and w_A resulting from the interaction of the incident sound wave with the unperturbed shock are therefore proportional to the incident sound field and of much smaller amplitude than the shock. This allows the linearization of the RH relations Eqs.(1-4). Substracting RH relations for the unperturbed shock front Eqs.(5-7) yields the linearized RH relations for mass

$$w_s(\rho_A^{inc} - \rho_P) + w_A(\rho_0 - \rho_s) = \rho_0 v_{A,x}^{inc} - \rho_s v_{P,x} - \rho_P v_s, \tag{31}$$

momentum in the shock normal direction x

$$\begin{aligned} &w_s \rho_0 v_{A,x}^{inc} - w_s \rho_s v_{P,x} - w_s \rho_P v_{s,x} - w_A \rho_s v_{s,x} \\ &\qquad = (p_A^{inc} - p_P) - 2\rho_s v_{s,x} v_{P,x} - \rho_P (v_{s,x})^2, \end{aligned} \tag{32}$$

momentum in the shock tangential direction y

$$v_{A,y}^{inc} = v_s \frac{\partial f}{\partial y} + v_{A,y}^{tr} + v_{E,y} + v_{V,y} , \tag{33}$$

and energy

$$\left(\frac{p_A^{inc}}{\rho_0} - \frac{p_P}{\rho_s}\right) - T_s s_P + w_s(w_A - v_{A,x}^{inc}) = (v_s - w_s)(v_P - w_A). \quad (34)$$

In all these linearized RH relations, one has to substitute the expressions of the various fields at the unperturbed shock position $x_s = w_s t$. In the same way as Snell-Descartes laws are usually established for acoustic refraction and reflexion through an interface, equalizing phase dependence versus space y provides the axial wavenumber of the various modes. Equalizing phase dependence versus time t yields the frequency of these modes behind the shock, and in particular the Doppler effect. The equalization of amplitudes leads to a four-by-four linear system for the four unknown amplitudes (T_A, T_E, T_V, T_W).

B. Doppler effect

Equalization of time dependencies yields

$$\begin{aligned} \omega - w_s k_{A,x}^{inc} &= \omega_A^{tr} - w_s k_{A,x}^{tr} \\ &= \omega_{E,V}\left(1 - \frac{w_s}{v_s}\right). \end{aligned} \quad (35)$$

pointing out the equality of frequencies of vorticity and entropy modes. The Doppler ratios between the frequencies of the modes behind the shock to the frequency of the incident sound wave

$$D_V = \frac{\omega_E}{\omega} = \frac{\omega_V}{\omega} = \frac{v_s(c_0 + w_s \cos\theta)}{c_0(v_s - w_s)} . \quad (36)$$

$$D_A = \frac{\omega_A^{tr}}{\omega} = \frac{c_0 + w_s \cos\theta}{c_0(1 - w_s r_{A,x}^{tr})}. \quad (37)$$

C. Regimes of refraction

Injecting Eq.(37) into the acoustical dispersion relation Eq.(22) shows that the x-component of the transmitted slowness vector is a root of a 2nd degree polynomial

$$\begin{aligned}\left(r^{tr}_{A,x}\right)^2 \left[(c_0 + w_s\cos\theta)^2(c_s^2 - v_s^2) + c_s^2 w_s^2 \sin^2\theta\right] \\ + 2\ \left[v_s(c_0 + w_s\cos\theta)^2 - w_s c_s^2 \sin^2\theta\right] r^{tr}_{A,x} \\ = (c_0 + w_s\cos\theta)^2 - c_s^2\sin^2\theta. \quad (38)\end{aligned}$$

Its solutions are

$$r^{tr}_{A,x} = \frac{w_s c_s^2 \sin^2\theta - v_s(c_0 + w_s\cos\theta)^2 \pm \sqrt{\Delta}}{(c_s^2 - v_s^2)(c_0 + w_s\cos\theta)^2 + (c_s w_s \sin\theta)^2} \quad (39)$$

with the associated discriminant Δ

$$\begin{aligned}\Delta = {} & (c_0 + w_s\cos\theta)^2 c_s^2 \\ & \times \left[(c_0 + w_s\cos\theta)^2 + \sin^2\theta((w_s - v_s)^2 - c_s^2)\right].\end{aligned} \quad (40)$$

In the absence of shock wave ($\epsilon = 0$ implying $v_s = 0$ and $w_s = c_s = c_0$), the solution of Eq.(39) with positive sign reduces to $r^{tr}_{A,x} = 1/c_0$ and the one with negative sign negative one to $r^{tr}_{A,x} = -\cos\theta/c_0$, which is the physical solution (unperturbed incident wave). Therefore, only solutions with negative sign in Eq.(39) are considered further. At normal incidence, it has the simple solution

$$r^{tr}_{A,x}(\theta = 0) = \frac{1}{v_s - c_s} \quad (41)$$

describing a wave counter-propagating at sound speed $-c_s$ and convected by the ambient flow v_s. In this case, the acoustical Doppler frequency shift is

$$D_A = \frac{\omega_A^{tr}}{\omega} = \frac{(c_0 + w_s)(c_s - v_s)}{c_0(w_s + c_s - v_s)}. \tag{42}$$

The transmitted frequency is larger (resp. smaller) than the incident one under the condition $c_s - v_s > c_0$ (resp. $c_s - v_s < c_0$) that the phase speed of the transmitted wave is larger (resp. smaller) than the incident one. Using expansions Eqs.(11,15,16) one gets

$$D_A = 1 + \frac{\epsilon}{4}\left(\frac{B}{A} - 2\right) + \frac{\epsilon^2}{32}\left(12 - \frac{10B}{A} + \frac{4C}{A} + \left(\frac{B}{A}\right)^2\right). \tag{43}$$

In particular, in the weak shock limit (second-order expansion), the transmitted frequency will be larger than the incident one ($D_A > 1$) for fluids with a nonlinear parameter larger than one ($B/2A > 1$), and smaller ($D_A < 1$) otherwise ($B/2A < 1$). This opposite behavior for fluids with a nonlinear parameter smaller (like air) or larger (like water) than one, will turn out essential to explain most features here investigated. This difference is due to the fact that the acoustical phase speed behind the shock is either larger or smaller than ahead of it.

A tedious asymptotic expansion up to order ϵ only yields

$$c_0 r_{A,x}^{tr} = -\cos\theta + \epsilon\left[\frac{3B}{4A} - \cos\theta\left(1 + \frac{B}{4A}\right)\right] + O(\epsilon^2). \tag{44}$$

In particular, at normal incidence one recovers $c_0 r_{A,x}^{tr} = -1 + \epsilon(\beta - 2)$ which is the weak shock limit of the slowness $1/(v_s - c_s)$. Injecting Eq.(44) in Eq.(37) gives

$$D_A = 1 + \frac{\epsilon}{1 + \cos\theta}\left[\frac{3B}{4A} - \cos\theta\left(1 + \frac{B}{4A}\right)\right] + O(\epsilon^2), \tag{45}$$

from which one deduces

$$\begin{aligned} k_{A,x}^{tr} &= \omega D_A s_{A,x}^{tr} \\ &= k_x + \frac{\omega}{c_0}\frac{\epsilon}{1 + \cos\theta}\left[\frac{3B}{4A} - \cos\theta\left(1 + \frac{B}{4A}\right)\right] + O(\epsilon^2). \end{aligned} \tag{46}$$

Eq.(46) brings light on the deviation of the transmitted wave, by introducing the function $g(\theta) = 3B/4A - \cos\theta(1 + B/4A)$ and by recalling that the incident wavenumber in the x-direction $k_x = -\omega\cos\theta/c_0$ is negative. The function g is equal to $B/2A - 1$ at normal incidence, so once again has a different sign for air and for water. At grazing incidence it is equal to $3B/4A$ which is assumed to be always positive. In the case $B/2A > 1$, the correction $g(\theta)$ is always positive: the angle of the transmitted wave with respect to the shock normal is always larger the incident one. Everything happens similarly to the usual linear Snell-Descartes laws with a transmission medium having a sound speed larger than than the incident one. This is called the 'normal' case, as the sound speed behind the shock is indeed larger than in the undisturbed medium, see Fig.(2.a). In the second case $B/2A < 1$, we observe the opposite behavior, see Fig.(2.b): the transmitted wave is propagating closer to the shock normal direction than the incident wave. This case is similar to the usual linear Snell-Descartes laws with a transmission medium having a sound speed *smaller* than the incident one. Such a refraction is observed here because the moderate increase in sound speed due to the shock with a moderate value of $B/2A < 1$, is counterbalanced by the convection due to post-shock flow motion in the opposite direction. However, this situation cannot be observed for all angles. Indeed function $g(\theta)$ can vanish at some neutral angle θ_0 defined by

$$\cos\theta_0 = \left(\frac{3B}{4A}\right) \Big/ \left(1 + \frac{B}{4A}\right), \tag{47}$$

which has a solution only if its right hand side is smaller than one, e.g. if $B/2A < 1$. At neutral angle θ_0, the wave is not deviated by the shock wave. Above it, function g is again positive and we recover a 'normal' deviation illustrated by Fig.(2.a). So for fluids such that

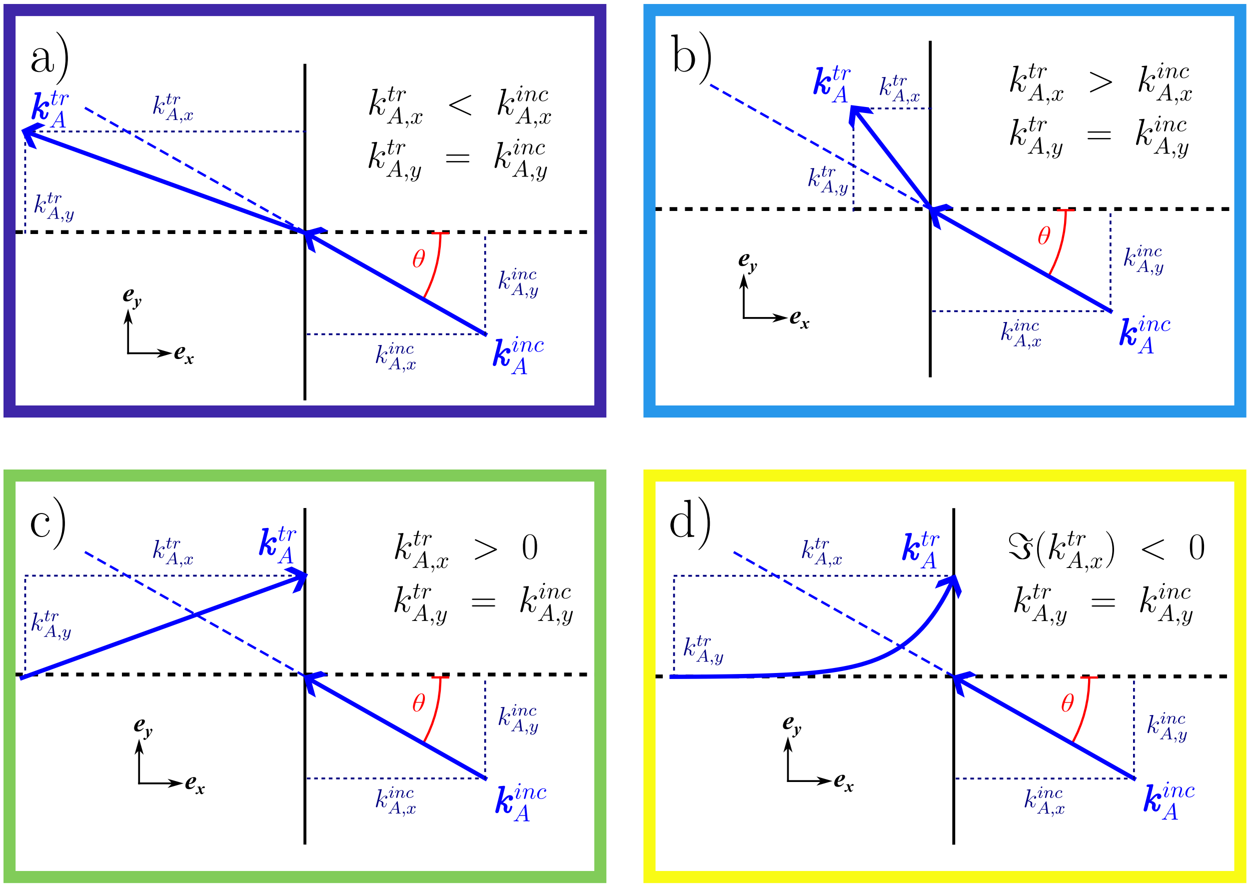

FIG. 2. Scheme illustrating properties of the different regimes of sound transmission. Dark blue : abnormal transmission - Light blue : normal transmission - Green : inverted transmission - Yellow : critical transmission. $k^{tr}_{A,x}$ is negative in the first two cases, positive in the last two ones.

$B/2A < 1$, we have first an 'abnormal' deviation for angles smaller than the neutral one, and then a 'normal' deviation for higher values. The neutral angle, if it exists, is (at least in the weak shock approximation) dependent on the medium, but independent on the shock amplitude (provided this one keeps sufficiently small).

Near grazing incidence, the axial slowness $r^{tr}_{A,x}$ can vanish. This happens for angles larger than a so-called inversion angle θ_I for which $r^{tr}_{A,x} = 0$, such that

$$\cos^2\theta_I(w_s^2+c_s^2)+2c_0w_s\cos\theta_I+c_0^2-c_s^2=0. \tag{48}$$

Solution of this second order polynomial in $\cos\theta_I$ is

$$\cos\theta_I=\frac{c_s\sqrt{c_s^2+w_s^2-c_0^2}-c_0w_s}{w_s^2+c_s^2}, \tag{49}$$

and using weak shock expansion we get

$$\theta_I=\frac{\pi}{2}-\epsilon\frac{B}{2A}. \tag{50}$$

This expression indicates that the angle of inversion deviates from grazing incidence proportionally to the weak shock amplitude ϵ and to its nonlinear parameter $B/2A$. Exactly at inversion angle, the transmitted wave propagates parallel to the shock front. For usual Snell-Descartes transmission, beyond this angle, one observes total reflexion. This cannot be the case here, because there is no reflected wave at all ! On the contrary, a transmitted wave still exists, but it now propagates *towards* the shock front instead of *away* from it. However, its speed in the axial direction x is much smaller than the shock velocity: the inverted transmitted wave cannot overtake the shock front and remains behind it. We call this regime 'inverted transmission', see Fig.(2.c).

At small incidences, discriminant Δ (Eq.(40)) involved in solution of axial slowness (Eq.(39)) is positive and solutions $r^{tr}_{A,x}$ are always real, leading to propagating waves. At grazing incidence $\theta=\pi/2=90°$, one has $\Delta=c_0^2c_s^2\left[c_0^2+(w_s-v_s)^2-c_s^2\right]$. The coefficient between brackets can potentially change of sign. Its asymptotic expansion is

$$\left[c_0^2+(w_s-v_s)^2-c_s^2\right]=1-\beta\epsilon-\Gamma\epsilon^2+O(\epsilon^3) \tag{51}$$

with $\Gamma=-1+B/2A+C/3A-D$. For not too small shock amplitudes ϵ and large values of Γ

such as those observed in water, it is possible that a weak shock leads to imaginary solutions for $r^{tr}_{A,x}$. This is called 'critical transmission'. Under the above quadratic approximation, the smallest shock amplitude at which this occurs is

$$\epsilon_C = \frac{\sqrt{\beta^2 + 4\Gamma} - \beta}{2\Gamma} \tag{52}$$

which for water is equal to about 0.088, reasonably small. In air, $\Gamma < 0$, preventing critical transmission for weak shock waves. This phenomenon is nevertheless observed for strong shocks[11]. For other materials, critical transmission will occur if coefficients of cubic nonlinearities are large enough compared to those of quadratic nonlinearities, so that $\Gamma > (\beta - \beta^2)/4$. However, this result should be taken with caution, as it ignores higher order terms in the various asymptotic expansions. In the general case (no weak shock approximation) the condition for critical transmission is $c_0^2 + (w_s - v_s)^2 - c_s^2 < 0$. The particular angle above which this kind of transmission is observed is called the critical angle θ_C.

As the critical transmission involves complex wavenumbers and frequencies, it raises the issue of stability of the flow in this case. This issue is handled in Appendix D, showing numerically that no instability arises.

To summarize (see Fig.(2), regarding geometry, there are four possible regimes of sound transmission through a moving weak shock. For a given medium, only three are possible : when $B/2A < 1$, the most frequent one is abnormal transmission. Normal transmission is observed for incidence angles larger than the neutral one, and inverted transmission at grazing angles and shocks not too weak. When $B/2A > 1$, the most common regime is normal transmission. When increasing incidence angle and shock strength, inverted transmission occurs and finally critical transmission.

D. Example : air versus water

These four regimes are illustrated by Fig.(3) for air (top line) and water (bottom line). The selected fluid properties are gathered in table I. For each medium, we used exact solution Eq.(39) to determine the transmitted wavenumber, but we used either (left column) low order (weak shock) quadratic expansions (first two terms in the r.h.s. of Eqs.(11,15,16) for the ambient shock parameters c_s, w_s, v_s), or (right column) higher order cubic ones for more precise results in the case of moderate shocks. The comparison allows to quantify the limit of the weak shock approximation. Shock amplitude ϵ ranges between 10^{-4} and 1, this last value being at the fringe of any asymptotic approximation. In air, explosions can lead to strong shocks with $\epsilon = 1$ or even much more. Sonic boom at the ground level produced by Concorde was of amplitude 100 Pa or $\epsilon = 7 \times 10^{-4}$. Future low boom aircraft are expected to induce significantly lower levels with $\epsilon \approx 10^{-4}$. In water, such value of ϵ corresponds to an easily reached amplitude of 0.225 MPa. Focused shocks produced by Extracorporeal Shock Wave Lithotripsy (ESWL)[26] can reach *in vitro* more than 100 MPa or $\epsilon \approx 4.6 \times 10^{-2}$. Intense laser focused on the surface of a metallic sample can produce observed velocity peaks of about 200 m/s in aluminum or titanium[27], corresponding to $\epsilon \approx 3 \times 10^{-2}$. The Hugoniot Elastic Limit (HEL) prevents the observation of much higher amplitudes without inducing irreversible plastic deformation[28]. Therefore, for liquids and solids, values much higher than 5×10^{-2} seem unlikely contrarily to air, but are nevertheless inspected here from a theoretical point of view.

TABLE I. Considered water, air and aluminum properties

	ρ (kg m^{-3})	c_0 (m s^{-1})	β	B/A	D	$C/(6A)$	K
Water	1000	1481	3.5	4.96	0.05	36.95	37.00
Air	1.2	340	1.2	0.4	0.08	-0.04	0.04
Alum.	2.7	6400	15[29]	28	0.05	375[29]	375.05

In air, the most common regime is the abnormal one (dark blue in Fig.(3)), observed for all amplitudes and all angles below θ_0 (plotted as a white dotted line). This one deviates from the constant value of Eq.(47) only when $\epsilon > 10^{-1}$. This quantifies the maximum value of low order weak shock approximation. Above, θ_0 is no more constant and tends to increase with ϵ considering third-order theory. For higher incidence angles, the normal regime (light blue) is observed. A tiny region for inverted transmission (green) appears at angles significantly different from 90° only for $\epsilon > 0.1$. In this case, it is more accurate to consider a 3rd-order expansion.

In water, the most common regime is normal transmission (light blue). Inverted transmission is observed in a much larger domain than in air, with significant deviation from 90° for $\epsilon > 0.01$. Third order expansion also predicts this regime at lower incidence than second order theory, for instance at about 50° for $\epsilon = 0.1$. Further increasing the shock amplitude soon leads to the regime of critical reflexion (yellow). This one is observed above $\epsilon \approx 0.2$ according to second order theory, but $\epsilon \approx 0.08$ according to third order theory. This last value is not very different from the approximation Eq.(52). When ϵ approaches one,

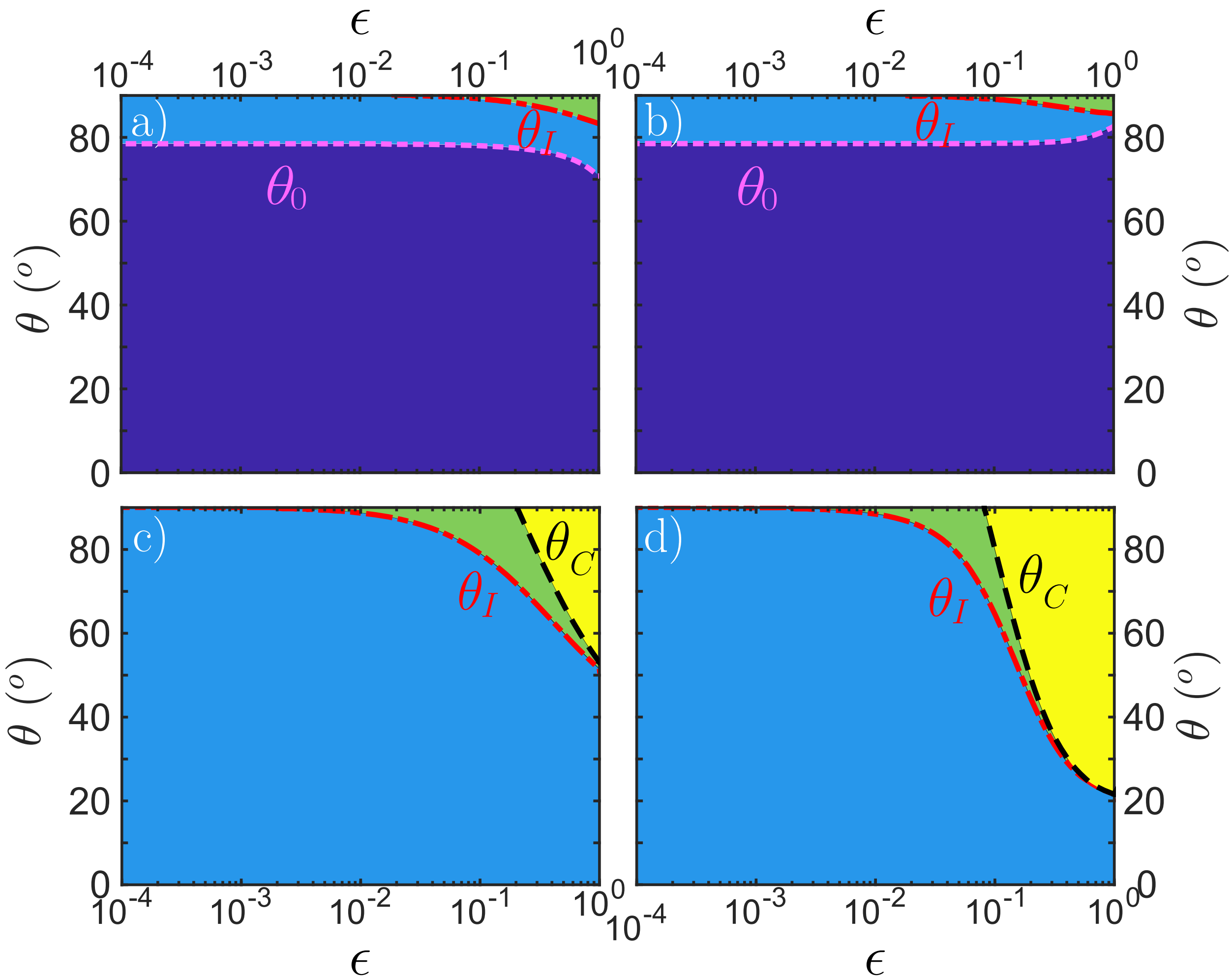

FIG. 3. Regimes of transmission for air (top line) and water (bottom line) depending on incidence angle θ and shock amplitude ϵ. Left (resp. right) column : results from second-order (resp. third-order) expansion of weak shock parameters. Dark blue : abnormal transmission - Light blue : normal transmission - Green : inverted transmission - Yellow : critical transmission

third-order theory also predicts critical transmission at much lower incidence angles than second-order one.

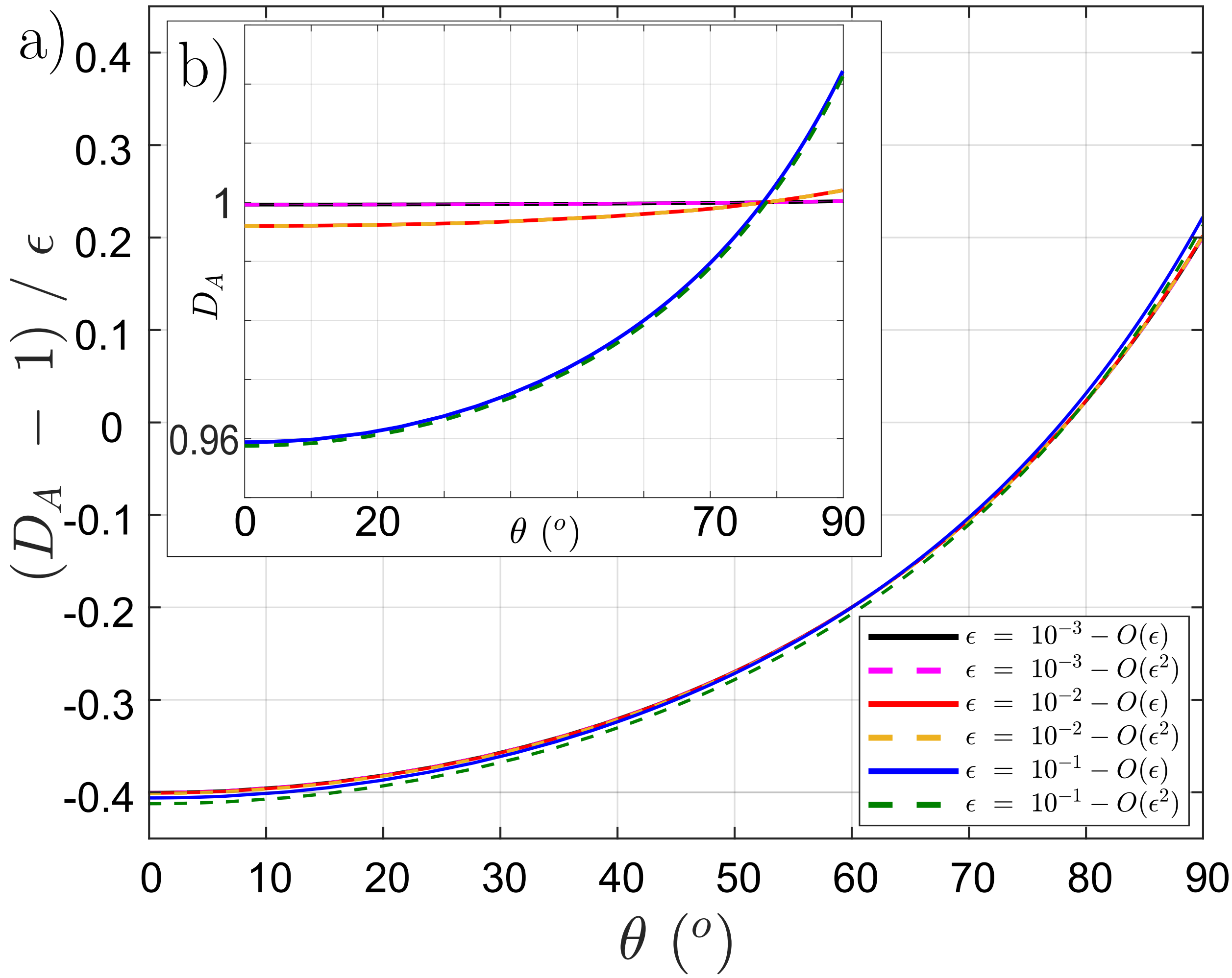

FIG. 4. Acoustical Doppler effect D_A for air (subfigure b)) and its normalized deviation from unity $(D_A - 1)/\epsilon$ (main figure a)) versus incidence angle for three shock amplitudes. Solid lines: 2nd-order theory. Dashed lines: 3rd-order one.

E. Doppler effects

Results for the Doppler ratio D_V are detailed in appendix C as they do not differ significantly between air and water and between 2nd and 3rd-order theories. Regarding the acoustic Doppler ratio, D_A is calculated using Eq.(37) for air (Fig.(4)) and water (Fig.(5)), also showing its deviation to unity normalized by shock amplitude $(D_A - 1)/\epsilon$. For air,

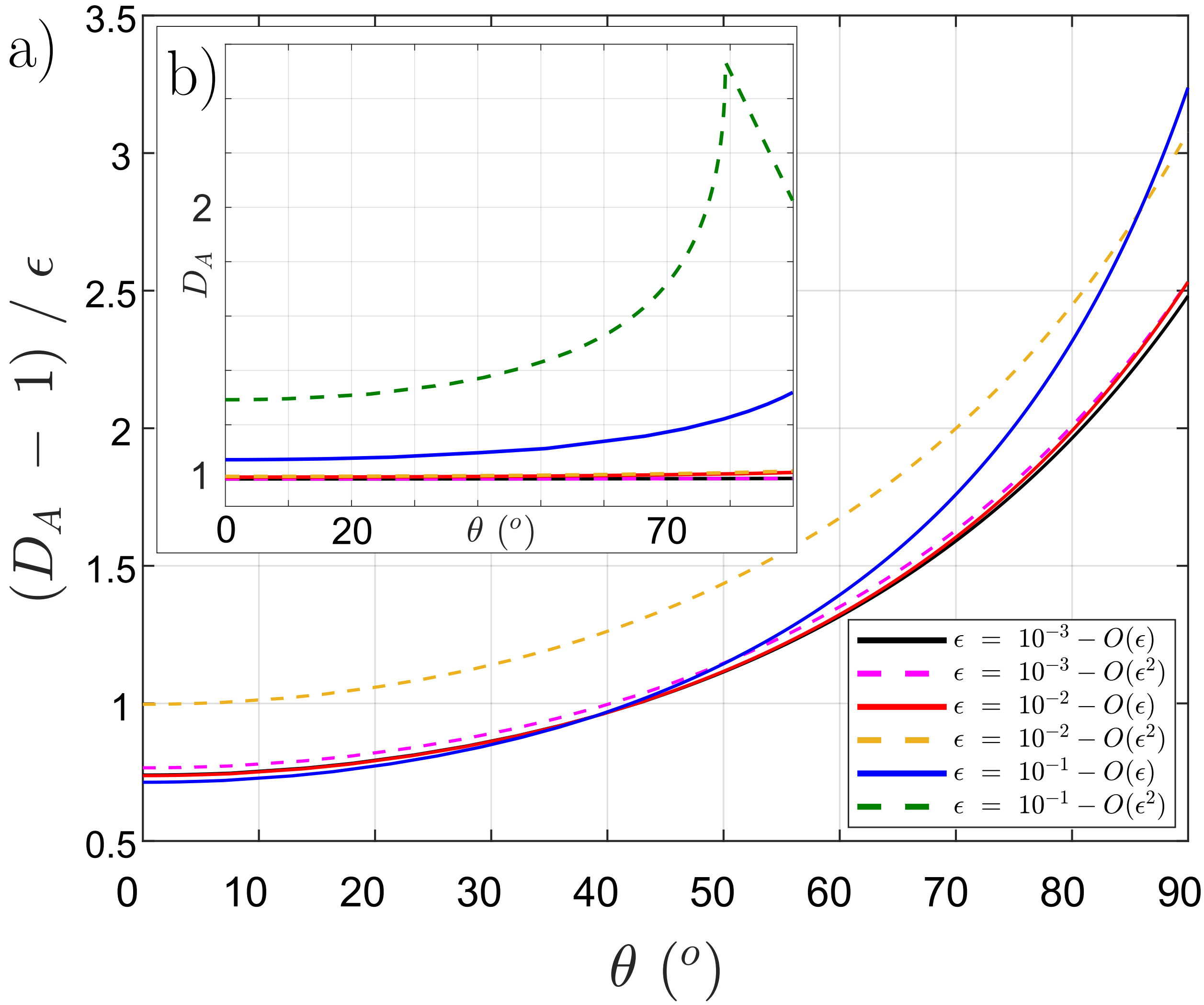

FIG. 5. Same as Fig.(4) for water. In subfigure a) the case $\epsilon = 10^{-1}$ for 3rd order theory is beyond range.

all curves almost superimpose, again showing weak shock theory is sufficient for prediction up to $\epsilon = 0.1$. Also D_A reaches the value of one at the neutral angle, for which the wave is not deviated nor its frequency changed. Above this angle, the transmitted frequency is increased, as we go from abnormal to normal transmission. For water, there is no abnormal regime and the acoustic frequency always increases through transmission. The Doppler effect is all the more important as the incidence angle is larger. Significant deviation between second- and third-order theories is visible even for the low strength $\epsilon = 10^{-2}$ due to the large value of $C/6A$. For $\epsilon = 10^{-1}$, the difference between the two orders is dramatic, with a much higher Doppler effect according to third order theory. In addition, this one predicts critical reflexion for an incidence angle larger than $\theta_C = 79.32°$, corresponding to a peak value of D_A. Beyond this incidence, D_A gets complex, but only its real part is plotted here.

V. AMPLITUDES

A. Linear system

Amplitudes (T_A, T_V, T_E, T_W) of each unknown wave are determined by the linearization of the four Rankine-Hugoniot shock relations. Introducing a function $f_s = c_s \sin\theta/(c_0 + w_s \cos\theta)$ and the density ratio $r_s = \rho_s/\rho_0$, one gets a four-by-four matrix system

$$(w_s - v_s - c_s n^{tr}_{A,x})T_A + w_s(r_s - 1)T_W + (w_s - v_s)T_E + f_s(v_s - w_s)T_V = w_s + c_0\cos\theta \tag{53a}$$

$$\frac{c_s \sin\theta}{c_0 D_A}(c_s + v_s n^{tr}_{A,x})T_A - \frac{r_s v_s w_s f_s}{c_s}T_W + c_s T_V = r_s c_0 \sin\theta \tag{53b}$$

$$\begin{aligned}(c_s^2 + v_s^2 - v_s w_s + c_s n^{tr}_{A,x}(2v_s - w_s))T_A - r_s v_s w_s T_W +\\ v_s(v_s - w_s)T_E + f_s(w_s - 2v_s)(v_s - w_s)T_V = c_0(c_0 + w_s\cos\theta)\end{aligned} \tag{53c}$$

$$c_s\left(c_s + (v_s - w_s)n^{tr}_{A,x}\right)T_A - r_s w_s v_s T_W - f_s(v_s - w_s)^2 T_V - c_s^2 r_s \frac{T_s}{T_0}\frac{\beta}{6D}T_E = c_0 r_s(c_0 + w_s\cos\theta) \tag{53d}$$

solved numerically to monitor the dependence of the transmission coefficients with incidence angle θ, shock strength ϵ and medium parameters.

B. Normal incidence

In the case of normal incidence $\theta = 0$ and second-order theory, the above system simplifies into a much simpler two-by-two system as vorticity mode vanishes. As shock entropy jump is of order ϵ^3 only, the amplitude of the entropy mode induced by the sound wave cannot exceed the ambient entropy increase so that $T_E = O(\epsilon^3)$. Therefore, everything happens at leading order as if the propagation were adiabatic, and energy RH relation can be omitted. This is detailed in Appendix B. The results

$$T_A = 1 + (1 - B/2A)\epsilon + O(\epsilon^2) \tag{54}$$

$$T_W = (B/2A - 1) + O(\epsilon) \tag{55}$$

once again outline the key effect of parameter $B/2A - 1$. If negative (resp. positive), the amplitude of the transmitted acoustic wave is larger (resp. smaller) than the incident one and the shock perturbation is in phase opposition (resp. in phase) to the incident wave. Comparison between 2nd- to 3rd-order theories in Fig.(6) shows the transmission loss (or gain) normalized by the shock strength ϵ $(T_A - 1)/\epsilon$. Results are shown for air, water and aluminum. In this last case (see values of parameters in Tab.(I)), we use the equivalence between nonlinear compression waves in fluids and solids[30]. Much higher values are found for β in case of solids. However, cubic nonlinear parameters are known for only few metals[29]. A deviation from the weak shock limit Eq.(54) is visible for air, as expected, only for relatively large shock amplitudes ($\epsilon > 0.1$). For water or aluminium, deviations are significant for much weaker shocks, namely $\epsilon \approx 0.01$, due to the large values of the high-order nonlinear parameters. This indicates that transmission of an acoustic wave through a weak shock can provide quantifiable information on higher-order nonlinear parameters of this kind of materials even at relatively small shock amplitudes of order $\epsilon = 10^{-2}$ experimentally achievable. Note also that, for aluminum and for a shock strength of $\epsilon = 10^{-2}$ corresponding to values reported in[27] for laser-generated shocks, Fig.(6) yields a transmitted amplitude reduced by about 10% relative to the incident one, in agreement with the experimental observations[21].

C. Oblique incidence

At oblique incidence, Fig.(7) illustrates the normalized transmission coefficients versus incidence angle for three shock strengths $\epsilon = 10^{-1}$, 10^{-2} and 10^{-3} in air. In water, Fig.(8) shows only the cases $\epsilon = 10^{-2}$ and 10^{-3}. The case $\epsilon = 10^{-1}$ with complex coefficients associated to critical reflexion examined separately. For both fluids, second- and third-order theory are shown. For acoustics, we plot transmission loss or gain normalized by shock amplitude $(T_A - 1)/\epsilon$. For the entropy mode, the coefficient T_E is normalized by the shock entropy jump ϵ^3 as it cannot be of larger order. The same normalization is chosen for the vorticity mode amplitude, while the shock perturbation is directly proportional to the sound wave. In air, all curves for acoustical transmission are quite similar : 2nd-order weak shock theory remains valid for all explored shock strengths and incidence angle and 3rd-order expansion provides only minor corrections. The sound amplification is essentially proportional to the shock amplitude. Whatever the angle, the wave amplitude is increased through transmission ($T_A > 1$). In particular, at the neutral angle θ_0 the sound wave is not deviated, but it is amplified. This amplification however reduces somewhat when increasing

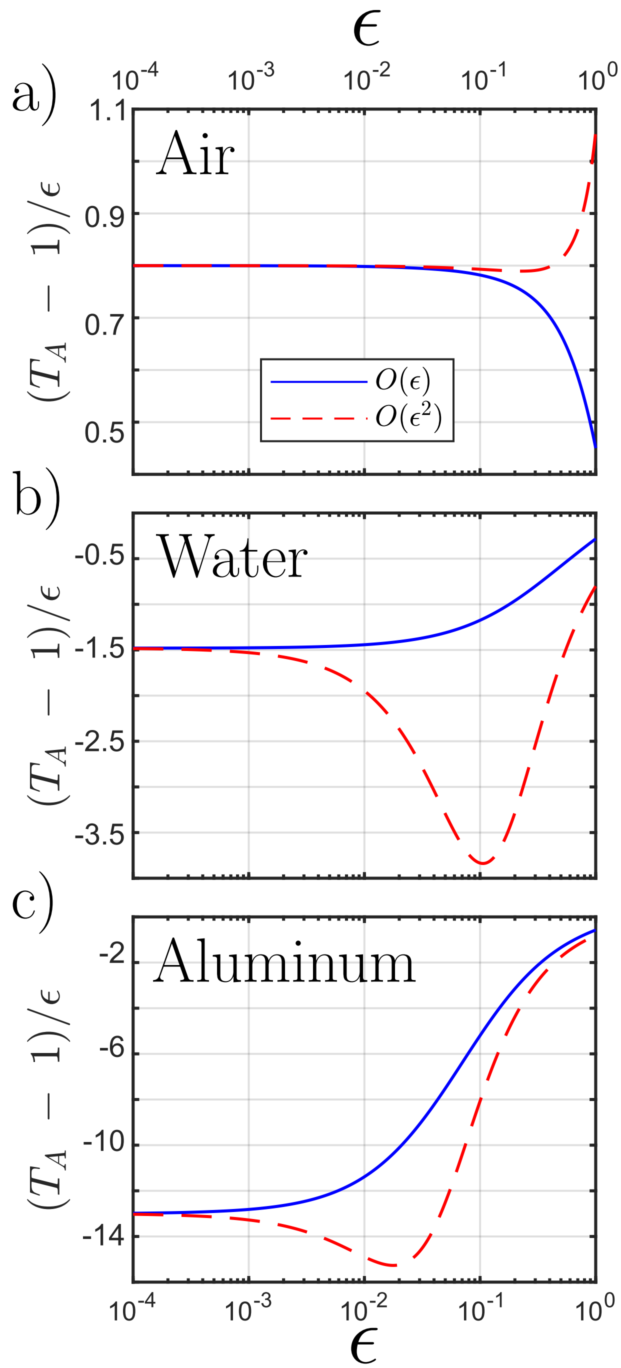

FIG. 6. Normalized transmission $(T_A - 1)/\epsilon$ coefficient at normal incidence ($\theta = 0°$) in the case of a) air, b) water c) and aluminum versus shock strength ϵ - second- (resp. third-) order theory in blue (resp. in red).

the incidence angle, reaches a minimum slightly below 60°, and then quickly increases above. As a counterpart, the amplitude of the shock perturbation, in phase opposition ($T_W < 0$) with the ambient shock, decreases in absolute value with angle, reaches a zero value at some particular angle around 75° independent on the shock amplitude, and then gets in phase ($T_W > 1$) with the shock at higher incidence. The very different behaviors of T_E and T_V depending on the theory order were to be expected at least for T_E : as both are of very small amplitude ϵ^3, second-order theory is insufficient to predict them accurately. From third-order theory, one observes that the amplitude of the vorticity mode varies in a non-monotonic way with angle, reaches a maximum in absolute value at around 65° and then decreases. On the contrary, the amplitude of the entropy mode shows little variations. Both modes tend to vanish near grazing incidence.

In water, see Fig.(8), as in air, the entropy and vorticity modes both remain very small and are poorly predicted by second-order theory. However, considering third-order theory, they are of opposite sign compared to air, and T_V increases significantly with incidence angle. Contrarily to air, the acoustic to entropy/vorticity is thus maximum at grazing incidence. The shock amplitude T_W is always positive (shock perturbation in phase with the incident wave) and is increasing with grazing angle, with a significant difference between second- and third-order theory visible above $\epsilon \approx 10^{-2}$. This difference is also visible for the normalized transmission coefficient $(T_A - 1)/\epsilon$ which is also increasing with angle. Thus, it changes of sign for angles around 77.24° (at $\epsilon = 10^{-2}$): we observe an amplitude decrease of the transmitted sound wave for small and moderate angles, and an increase for large ones. Note this amplitude change occurs at smaller values that the inverted transmission.

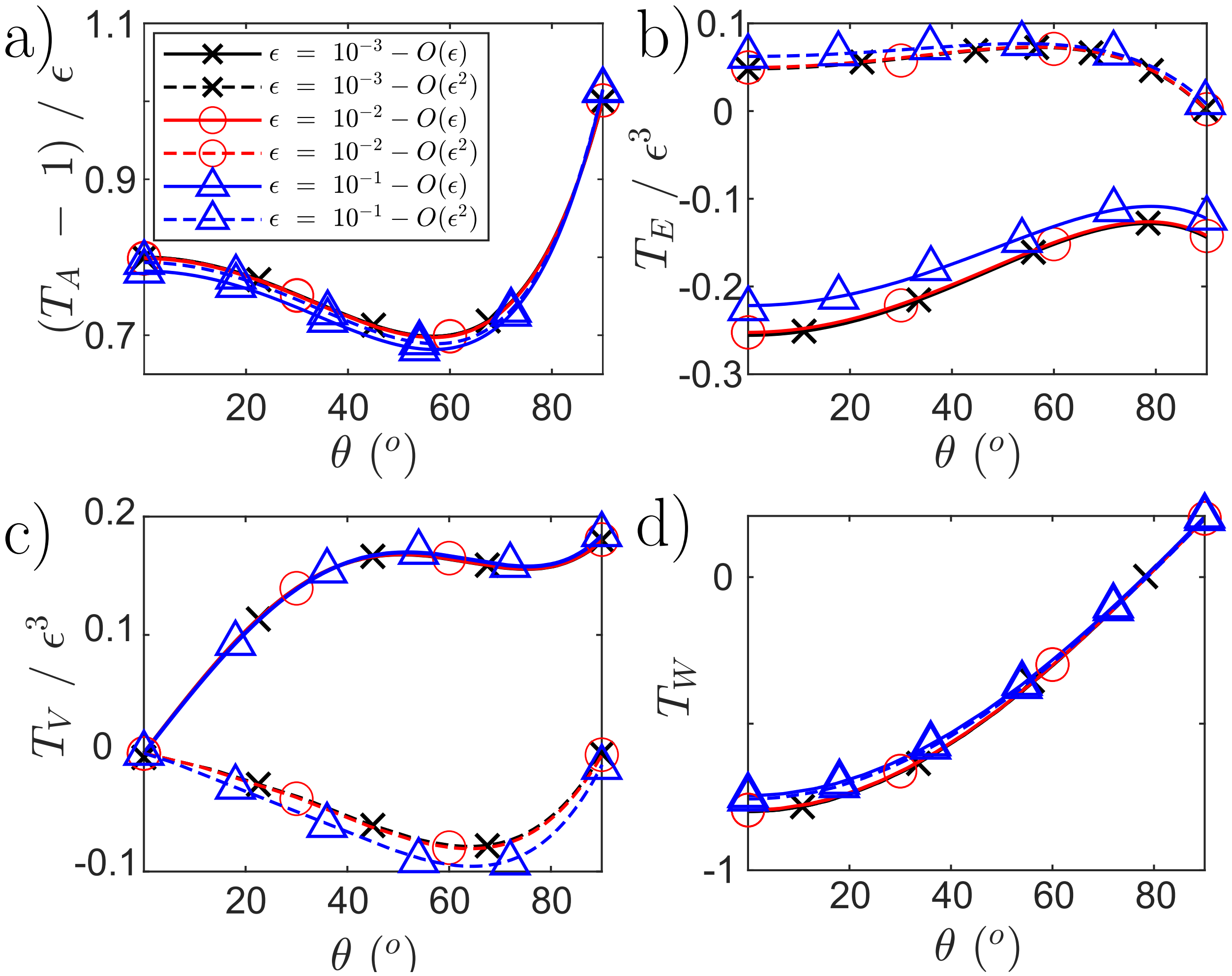

FIG. 7. Normalized angular variations of the transmission coefficients in the case of air for three different shock strengths $\epsilon = 10^{-3}$ (black), $\epsilon = 10^{-2}$ (red) and $\epsilon = 10^{-1}$ (blue). Second-order theory (solid lines) is compared to third-order one (dashed lines).

As noticed in Fig.(3) for water and $\epsilon = 0.1$, critical reflexion beyond angle θ_C is predicted (by third-order theory), leading to complex values above this angle. This case is shown on Fig.(9). The critical angle is here $\theta_C = 79.32°$. Below it, all transmission coefficients show the same behavior observed in water for smaller shock strengths, and increase (in absolute value - note that only T_E is negative) with incidence angle. This increase accelerates when

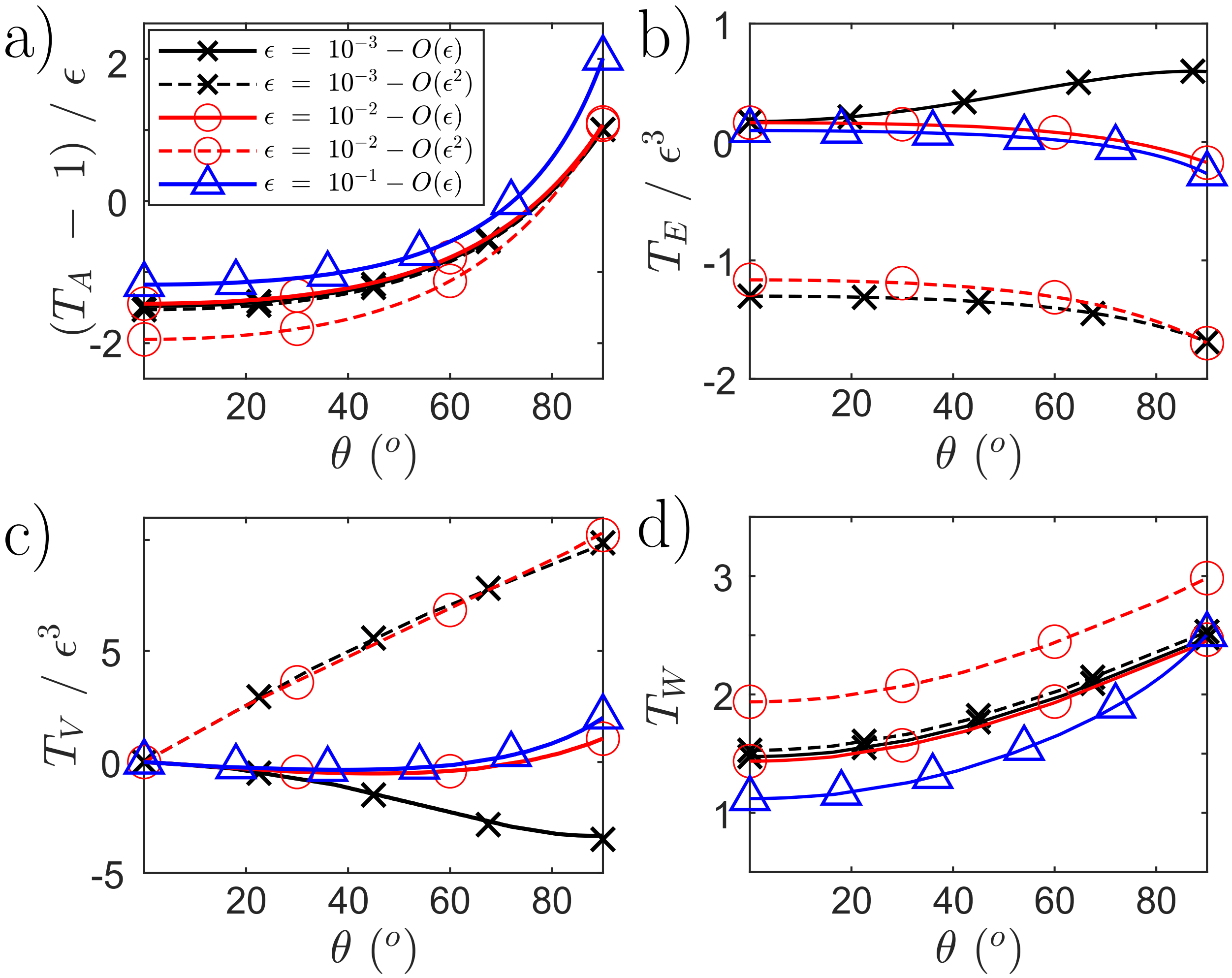

FIG. 8. Same as Fig.(7) for water. The case $\epsilon = 0.1$ is shown separately.

approaching the critical angle. Beyond the critical angle, all real parts sharply fall down, except the one of the vorticity mode that suddenly changes of magnitude, getting of order ϵ instead of order ϵ^3 for smaller angles. Above θ_C, all imaginary parts also brutally increase in absolute value before reaching a smoother variation. Such sharp variations were also observed for imaginary parts of frequency and wavenumber, see Fig.(11).

For the value $\epsilon = 10^{-0.5}$ closer to unity, the critical regime appears at a much smaller angle $\theta_C = \theta = 34.88°$. Below this value, compared to the case $\epsilon = 0.1$, real transmission

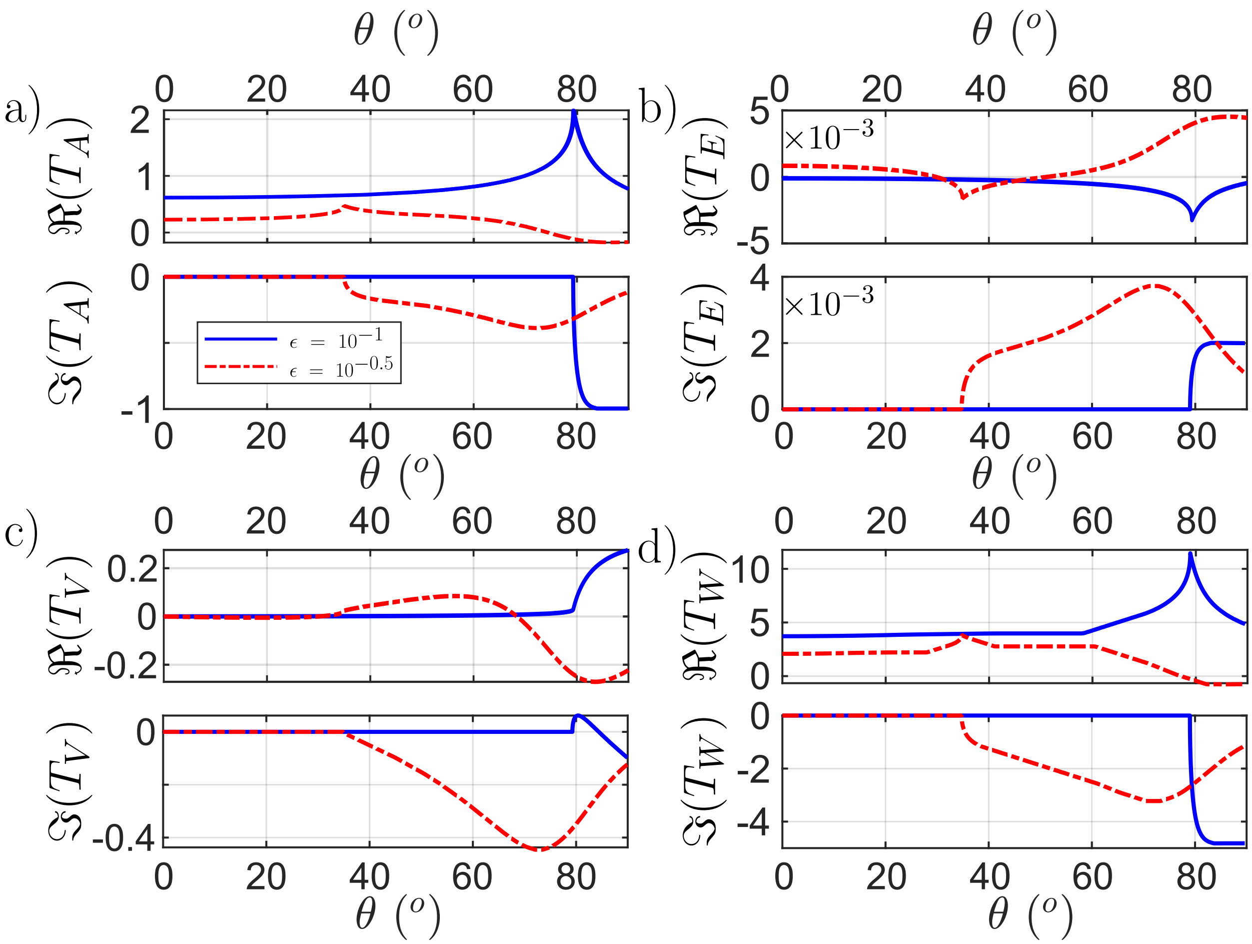

FIG. 9. Angular variation of the real and imaginary parts of transmission coefficients in the case of water for $\epsilon = 10^{-1}$ (blue solid line) and $\epsilon = 10^{-0.5}$ (red dashed line) for a 3rd-order expansion.

coefficients tend to be of smaller amplitude, except T_E which is no longer negligible and changes of sign. Beyond the critical angle, compared to $\epsilon = 0.1$, the variations of real and imaginary parts are not as sharp, values for T_A and T_W are smaller while those of T_V and T_E are larger. In this case at the fringe of asymptotic approximation, the energy of the incident wave tends to be more equally distributed among the four induced modes. This case approaches the configurations with stronger shocks studied in the literature (for air only).

VI. CONCLUSION

This study investigates the interaction between an acoustic wave and a counter-propagating weak shock wave. In contrast to previous studies, attention is focused to the case of weak shocks in the nonlinear acoustical limit. Second- and third- order expansions for the shock parameters are compared to quantify the limits of the weak shock approximation. The case of an ideal gas is extended to any common fluid, allowing the comparison of water versus and air. Several regimes of sound transmission have been highlighted, depending on the incidence angle, the shock strength and the nonlinear parameter(s) of the fluid. For most cases, air shows an 'abnormal' refraction with an angle of refraction smaller than the incident one because of the dominant effect of convection compared to the non-linearity of the state equation. On the contrary, water shows a normal behavior with a refraction angle larger than the incident one. When increasing the shock strength, normal refraction is recovered for air. For both fluids, an 'inverted' transmission regime is observed at high incidences for the highest considered shock strengths (in the case of a 'not too weak' shock), with a transmitted wave propagating towards the shock, while remaining slower. For water only, an evanescent wave is observed for highest amplitudes and largest incidence angle, but no shock instability is observed in the weak shock limit. Because third-order nonlinear parameters of their respective state equation are much higher for water than for air, significant differences are observed for water between second- and third-order theories, while differences are much tinier for air. Deviations of sound transmission coefficient from unity show significant differences between second- and third-order theories, even at relatively small shock strengths for water. Amplitudes of entropy and vorticity modes generally remain negligible, of order ϵ^3. This was expected for entropy due to the smallness of the shock entropy jump. However, for water, induced vorticity cannot be neglected anymore for the critical regime when transmitted sound wave gets evanescent. In all cases, the perturbation of the shock wave resulting from its interaction with the sound wave cannot be neglected. The present theory has to be extended in the future to the case of hyperelastic solids. For metals such as aluminum or titanium, we expect even stronger interactions due to the higher coefficients of non-linearity of their constitutive laws, in qualitative agreement with the recent experimental observations. This paves the way to a new measurement method of third-order elastic constants, in particular in solids, and to an *in situ* monitoring of shock propagation by ultrasound in opaque materials.

APPENDIX A: EXPRESSION OF COEFFICIENT D

Coefficient D can be determined by recalling the formula (see for instance appendix 2 of Ref.[31])

$$\left(\frac{\partial p}{\partial s}\right)_\rho = c_0^2 T_0 \left(\frac{1}{c_v} - \frac{1}{c_p}\right)\left(\frac{\partial \rho}{\partial T}\right)_s \tag{A1}$$

where $c_v = T_0(\partial s/\partial T)_\rho$ (resp. $c_p = T_0(\partial s/\partial T)_p$) is the specific heat capacity at constant volume (resp. at constant pressure), $\gamma = c_p/c_v$ being their ratio. We also have $T_0 = \left(\frac{\partial e}{\partial s}\right)_\rho$ and $p_0 = \rho_0^2\left(\frac{\partial e}{\partial \rho}\right)_s$ with e the specific internal energy. Maxwell relation gives $\left(\frac{\partial p}{\partial s}\right)_\rho = \rho_0^2\left(\frac{\partial^2 e}{\partial \rho \partial s}\right) = \rho_0^2\left(\frac{\partial T}{\partial \rho}\right)_s$. Multiplying the two expressions of $(\partial p/\partial s)_\rho$ gives

$$\left(\frac{\partial p}{\partial s}\right)_\rho = \rho_0 c_0 \sqrt{\frac{T_0}{c_v}}\sqrt{\frac{\gamma - 1}{\gamma}} \tag{A2}$$

and therefore

$$D = \frac{\beta}{6}\sqrt{\frac{c_0^2}{T_0 c_v}}\sqrt{\frac{\gamma-1}{\gamma}}. \tag{A3}$$

For a perfect gas of molar mass M_0 with d degrees of freedom (3 for monoatomic gases, 5 for diatomic ones) $c_v = dr/2$, $\gamma = (d+2)/d$ and $c_0 = \sqrt{\gamma r T_0}$ with $r = R/M_0$ (R being the universal gas constant). One gets $\left(\dfrac{\partial p}{\partial s}\right)_\rho = (\gamma-1)\rho_0 T_0/d$ and deduces $D = (\gamma^2-1)/12$ and $K = (\gamma-1)^2/4$, equal to respectively 0.08 and 0.04 for a diatomic gas. For water at 20°C with c_0 =1481m/s, c_v =4203 J/K/kg, γ =1.004 and β =3.5, one obtains D =0.05, much smaller than $C/6A$. For water, the effects of entropy jump are negligibly small compared to those of cubic, isentropic non-linearity , while they are comparable and of opposite signs for air.

APPENDIX B: TRANSMISSION COEFFICIENTS AT NORMAL INCIDENCE

At normal incidence, $\theta = 0$, $f_s = 0$, there cannot be any vorticity mode so that $T_V = 0$ and the wave direction is unchanged $n^{tr}_{A,x} = -1$. By introducing the new unknowns $X_A = (c_s - v_s + w_s)T_A$, $X_W = w_s T_W$, $X_E = (w_s - v_s)T_E$ and the notation $C = c_0 + w_s$, the 1D system Eqs.(53a-53d) can be rewritten

$$X_A + (r_s - 1)X_W + X_E = C \tag{B1a}$$

$$(c_s - v_s)X_A - r_s v_s X_W - v_s X_E = c_0 C \tag{B1b}$$

$$\tfrac{c_s}{r_s} X_A - v_s X_W - \tfrac{c_s^2}{w_s - v_s}\tfrac{T_s}{T_0}\tfrac{\beta}{6D} X_E = c_0 C \tag{B1c}$$

Inserting the expressions Eq.(11) for c_s , Eq.(16) for w_s and Eq.(15) for v_s but limited at second-order expansions yields

$$X_A + \epsilon X_W + X_E = C \tag{B2a}$$

$$(1 + \epsilon(\beta - 2))X_A - \epsilon X_W - \epsilon X_E = C + O(\epsilon^2) \tag{B2b}$$

$$(1 + \epsilon(\beta - 2))X_A - \epsilon X_W - \alpha X_E = C + O(\epsilon^2), \tag{B2c}$$

with $\alpha = \beta/6D + O(\epsilon)$. The last two equations are identical except for the coefficient in front of X_E. Substracting them, on gets that $X_E = O(\epsilon^2)$ at most, showing that the entropy mode has a much smaller amplitude than the other ones. Indeed, entropy induced by the incident sound wave cannot be bigger than the entropy jump through the unperturbed shock, and therefore one has necessarily $X_E = O(\epsilon^3)$. It can thus be ignored, and the system for (X_A, X_W) reduces to Eqs.(B2a-B2b). Solving it leads to $X_A = C(1-\epsilon(B/2A-1)/2+O(\epsilon^2))$ and $X_W = (B/2A - 1)/2 + O(\epsilon)$. Returning to physical variable yields Eqs.(54-55).

APPENDIX C: FREQUENCY OF VORTICITY AND ENTROPY MODES

The Doppler ratio D_V for vorticity and entropy modes, given by Eq. (36), is now considered for the same parameters and media. As D_V is proportional to the ambient flow velocity v_s, it is proportional to the dimensionless amplitude ϵ. This is a high to low frequency conversion from acoustics to vorticity/entropy. A first order expansion of Eq. (36) yields $D_V = -\epsilon(1 + \cos\theta) + O(\epsilon^2)$ independent of the medium parameters. Therefore Fig.(10) shows the ratio D_V/ϵ. As expected, results are quite insensitive to both shock strength and medium: the ratio increases with incidence angle from -2 at normal incidence to -1 at

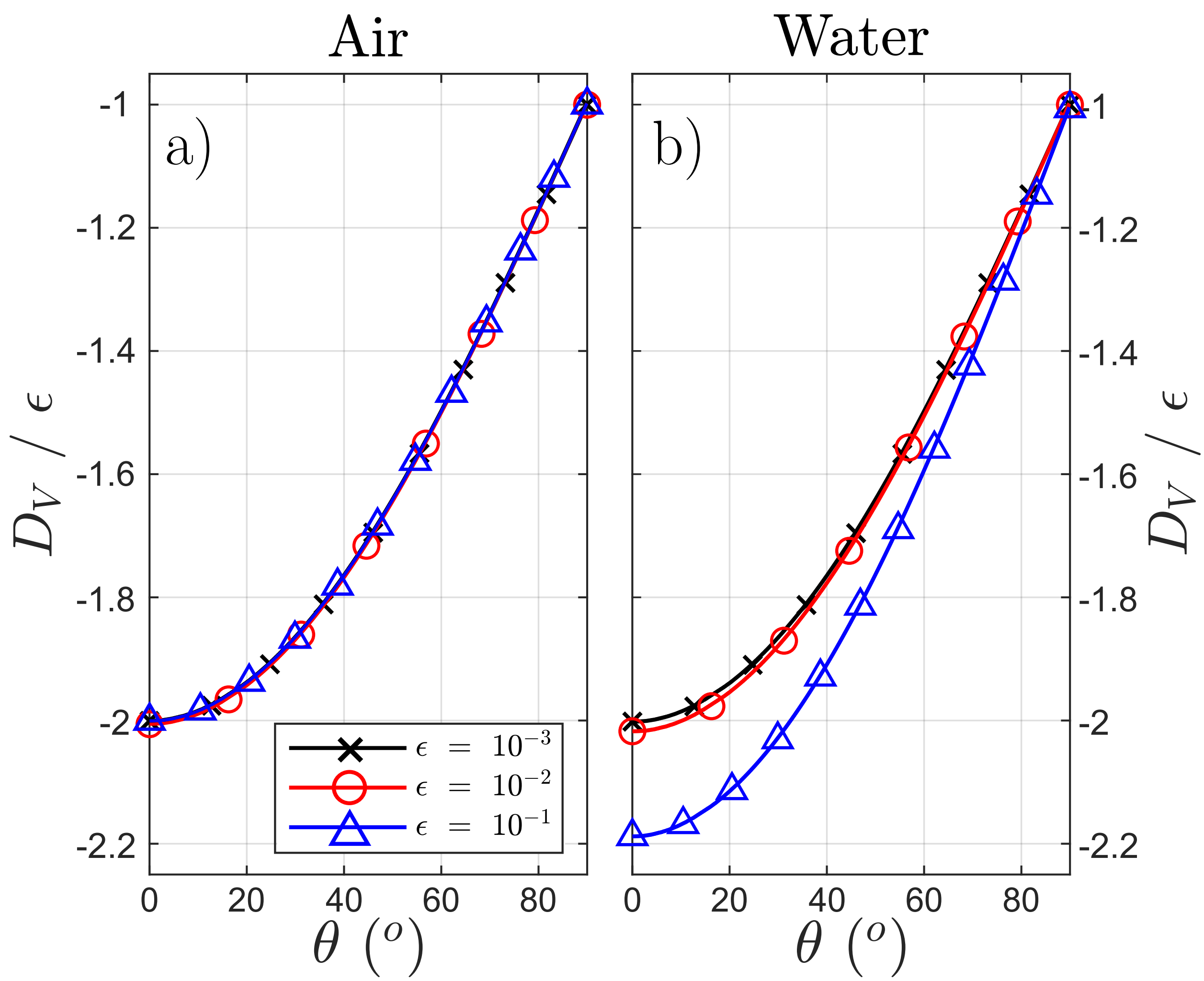

FIG. 10. Angular variation of the normalized Doppler ratio D_V/ϵ versus incidence angle for three shock amplitudes for a) air and b) water. Only 2nd-order theory is shown, differences with 3rd-order one are negligible.

grazing angles. Only the values for strongest shocks ($\epsilon = 10^{-1}$) in water (the medium with the highest nonlinear parameters) slightly vary by about 10%. Comparison between second- and third-order theories show negligible differences of order ϵ^3 for D_V.

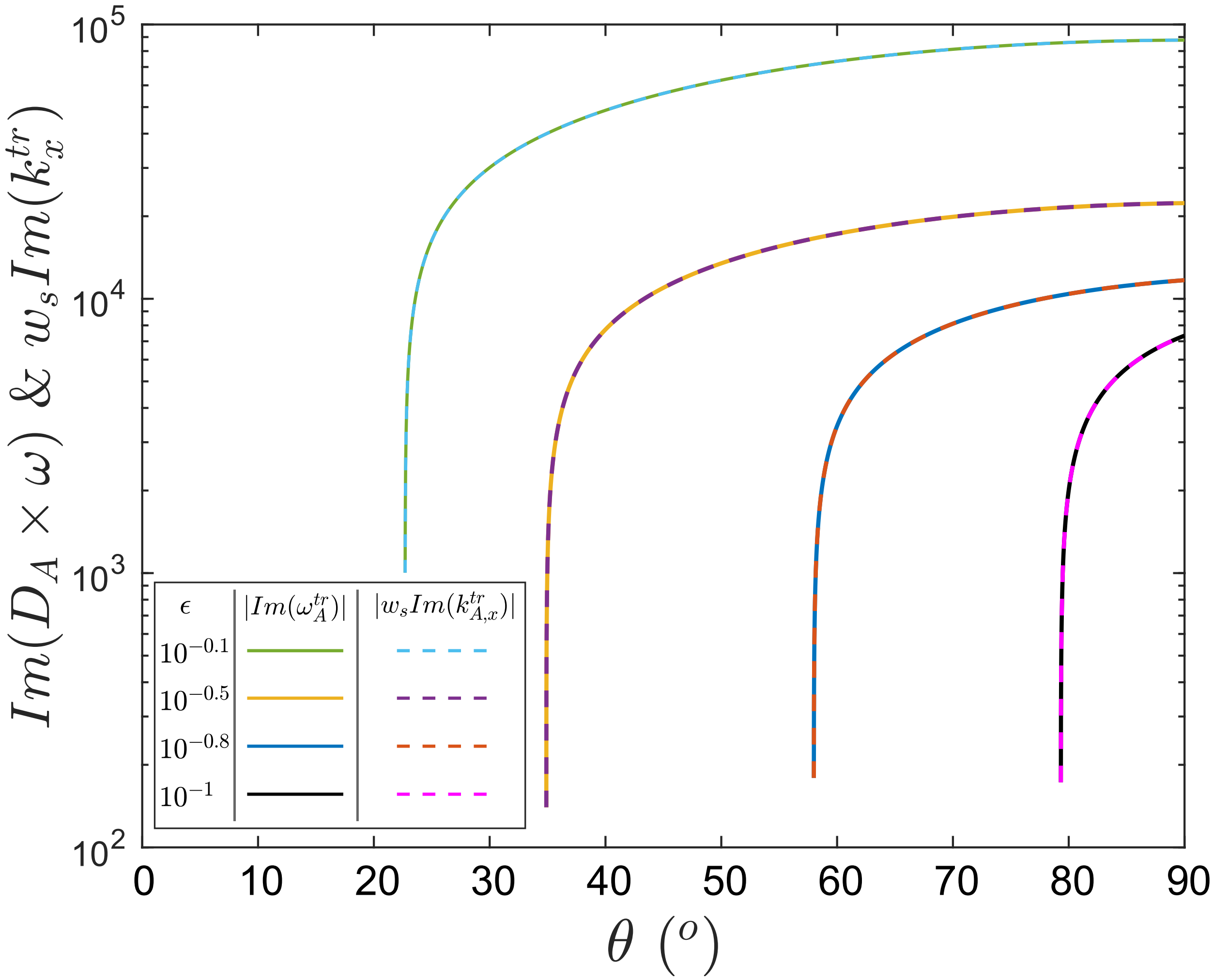

FIG. 11. Angular variation of (I_ω) and $(w_s I_k)$ in the case of water for four values of ϵ between 0.1 and 1, considering a third-order expansion.

APPENDIX D: FLOW STABILITY

As the critical transmission involves complex wavenumbers and frequencies, it raises the issue of stability of the flow in this case. In terms of density, the transmitted acoustic wave may be rewritten

$$\rho_A^{tr}(x,y,t) \;=\; AT_A \exp\left(j\left[R_k x \;+\; k_y y \;-\; R_\omega t\right]\right) \times \exp\left(I_\omega t \;-\; I_k x\right) \;. \tag{D1}$$

where R_k and I_k (resp. R_ω and I_ω) are the real and imaginary part of $k_{A,x}^{tr}$ (resp. of ω_A^{tr}). Spatial stability at large distances from the shock front $x \to -\infty$ is ensured by choosing the imaginary part of the complex wavenumber negative $I_k < 0$. However the shock is moving towards positive values of x at speed w_s, which could potentially induce an exponential growth of the solution. The most sensitive point is the shock front at position $w_s t$. At this point, the stability is determined by the term $\exp\left[\left(I_\omega \;-\; I_k w_s\right) t\right]$, which will be stable only if $I_\omega \;-\; I_k w_s \leq 0$. We found no simple way to evaluate analytically this quantity, so it was computed numerically using either second- or third-order expansions for water and for shock strengths ϵ large enough so that the critical transmission exists. Results are displayed in Fig.(11). Only results for third-order theory are shown as this one is better adapted to moderate (not too small) values of ϵ for which the critical regime is observed. Below θ_C, both I_k and I_ω are null and are not displayed due to the chosen logarithmic scale. Above θ_C, both I_k and $w_s I_\omega$ quickly increase (by one or two orders of magnitude) over the first couple of degrees, and then increase at a much slower pace. But the main result is that, for each tested value of ϵ, we find numerically that $I_k \;=\; w_s I_\omega$. When computing the difference between the two, we obtain equality close to the machine precision (roughly 10^{-11}), whatever the theory order we rely on. We can therefore conclude that the critical transmission does not induce a flow instability. The transmitted wave keeps bounded on the shock front where it reaches its maximum amplitude, while decaying exponentially with distance away from the shock. It is nevertheless associated to a real component of the axial wavenumber, and thus appears as an acoustical surface wave localized behind the shock front. This last regime is illustrated by Fig.(2.d).

Conflict of Interest

The authors have no conflicts of interest to disclose.

Data Availability

Data sharing is not applicable to this article as no new data were created or analyzed in this study.

References

[1] J. M. Burgers. On the transmission of sound waves through a shock wave. *Koninklijke Nederlandse Akademie van Wetenschappen*, XLIX:273–281, 1946.

[2] J. M. Burgers. On the transmission of sound waves through a shock wave. In F. T. M. Nieuwstadt and J. A. Steketee, editors, *Selected Papers of J. M. Burgers*, pages 478–486. Springer, Dordrecht, 1995.

[3] D. Blokhintzev. The propagation of sound in an inhomogeneous and moving medium ii. *The Journal of the Acoustical Society of America*, 18(2):329–334, October 1946.

[4] A. Kantrowitz. The formation and stability of normal shock waves in channel flows. Technical Report 1225, NACA, Langley, VA, 1947.

[5]F. K. Moore. Unsteady oblique interaction of a shock wave with a plane disturbance. Technical Report 2879, NACA, Cleveland, OH, 1953.

[6]J. Brillouin. Réflexion et refraction d'ondes acoustiques par une onde de choc. *Acta Acustica united with Acustica*, 5(3):149–163, January 1955.

[7]L. S. Kovásznay. Turbulence in supersonic flow. *Journal of the Aeronautical Sciences*, 20(10):657–674, 1953.

[8]W. G. Unruh. Experimental black-hole evaporation? *Physical Review Letters*, 46(21):1351–1353, 1981.

[9]O. Lahav, A. Itah, A. Blumkin, C. Gordon, S. Rinott, A. Zayats, and J. Steinhauer. Realization of a sonic black hole analog in a bose-einstein condensate. *Physical Review Letters*, 105(24):240401(1–4), 2010.

[10]J. Steinhauer. Observation of quantum Hawking radiation and its entanglement in an analogue black hole. *Nature Physics*, 12(10):959–965, 2016.

[11]J. F. McKenzie and K. O. Westphal. Interaction of linear waves with oblique shock waves. *The Physics of Fluids*, 11:2350–2362, 1968.

[12]A. N. Kudryavtsev and A. Yu Ovsyannikov. Numerical investigation of the interaction of acoustic disturbances with a shock wave. *TSAGI*, 41(1):47–57, 2010.

[13]J. F. McKenzie and K. O. Westphal. Transmission of Alfvén waves through the earth's bow shock. *Planetary and Space Science*, 17(5):1029–1037, 1969.

[14]V M Kontorovich. On the interaction between small disturbances and discontinuities in magnetohydrodynamics and on the stability of shock waves. *Soviet Physics JETP*,

35(5):851–858, May 1959.

[15]W. I. Axford, E. Leer, and G. Skadron. The acceleration of cosmic rays by shock waves. In *15th international cosmic ray conference - late papers*, volume 11, pages 132–137. Bulgarian academy of sciences, 1977.

[16]Y. Andreopoulos, J. H. Agui, and G. Briassulis. Shock wave—turbulence interactions. *Annual review of fluid mechanics*, 32(1):309–345, 2000.

[17]Y. Ma and X. Zhong. Receptivity of a supersonic boundary layer over a flat plate. part 2. receptivity to free-stream sound. *Journal of Fluid Mechanics*, 488:79–121, 2003.

[18]K. Mahesh, S. Lee, S. K. Lele, and P. Moin. The interaction of an isotropic field of acoustic waves with a shock wave. *Journal of Fluid Mechanics*, 300:383–407, 1995.

[19]A. Morro. Interaction of acoustic waves with shock waves in elastic solids. *Zeitschrift für angewandte Mathematik und Physik ZAMP*, 29:822–827–248, 1978.

[20]S. Pluchino. Interaction of a weak wave with a characteristic shock in a hyperelastic medium. *Meccanica*, 16:192–195, 1981.

[21]M. Ducousso, E. Cuenca, M. Marmonier, L. Videau, F. Coulouvrat, and L. Berthe. Bulk probing of shock wave spatial distribution in opaque solids by ultrasonic interaction. *Phys. Rev. Appl.*, 15(5):L051002(1–6), 2021.

[22]M. F. Hamilton and D.T. Blackstock. *Nonlinear Acoustics*. Academic Press, San Diego, 1998.

[23]S. Baskar, F. Coulouvrat, and R. Marchiano. Nonlinear reflection of grazing acoustic shock waves: unsteady transition from von neumann to mach to snell–descartes reflections.

Journal of Fluid Mechanics, 575:27–55, 2007.

[24]Philip A. Thompson. *Compressible-fluid Dynamics*. McGraw-Hill, 1972.

[25]A. B. Coppens, R. T. Beyer, M. B. Seiden, J. Donohue, F. Guepin, R. H. Hodson, and C. Townsend. Parameter of nonlinearity in fluids. ii. *The Journal of the Acoustical Society of America*, 38(5):797–804, 1965.

[26]R. O. Cleveland and J. A. McAteer. Physics of shock-wave lithotripsy. *Smith's textbook of endourology*, pages 527–558, 2012.

[27]E. Cuenca, M. Ducousso, A. Rondepierre, L. Videau, N. Cuvillier, L. Berthe, and F. Coulouvrat. Propagation of laser-generated shock waves in metals: 3D axisymmetric simulations compared to experiments. *Journal of Applied Physics*, 128(24):244903(1–13), 2020.

[28]G. I. Kanel, V. E. Fortov, and S. V. Razorenov. *Elastic-plastic response of solids under shock-wave loading*. Springer Science & Business Media, New York, NY, 2004.

[29]H. Sun and J. Zhu. Determination of acoustic nonlinearity parameters using thermal modulation of ultrasonic waves. *Applied Physics Letters*, 116(24), 2020.

[30]A. N. Norris. Finite-amplitude waves in solids. In M. F. Hamilton and D.T. Blackstock, editors, *Nonlinear acoustics*, chapter 9, pages 263–277. Academic Press, San Diego, 1998.

[31]F. Coulouvrat. On the equations of non linear acoustics. *Journal d'acoustique*, 5(4):321–359, 1992.